minerals

MDPI

Article

Industrial Ceramics: From Waste to New Resources for Eco-Sustainable Building Materials

Maura Fugazzotto [1], Paolo Mazzoleni [1,*], Isabella Lancellotti [2], Rachel Camerini [3], Pamela Ferrari [3], Maria Rosaria Tiné [4], Irene Centauro [5], Teresa Salvatici [5] and Germana Barone [1]

[1] Department of Biological, Geological and Environmental Sciences, University of Catania, Corso Italia, 57, 95129 Catania, Italy; maura.fugazzotto@unict.it (M.F.); gbarone@unict.it (G.B.)
[2] Department of Engineering "Enzo Ferrari", University of Modena and Reggio Emilia, Via Pietro Vivarelli, 10, 41125 Modena, Italy; isabella.lancellotti@unimore.it
[3] Center for Colloid and Surface Science (CSGI) and Department of Chemistry, University of Florence, Via Della Lastruccia, 3, 50019 Sesto Fiorentino, Italy; camerini@csgi.unifi.it (R.C.); pamelaferrari.84@gmail.com (P.F.)
[4] Department of Chemistry and Industrial Chemistry, University of Pisa, Via Giuseppe Moruzzi, 13, 56124 Pisa, Italy; mariarosaria.tine@unipi.it
[5] Department of Earth Science, University of Florence, Via La Pira, 4, 50121 Firenze, Italy; irene.centauro@unifi.it (I.C.); teresa.salvatici@unifi.it (T.S.)
* Correspondence: pmazzol@unict.it

Abstract: Today, the need to dispose of a huge amount of ceramic industrial waste represents an important problem for production plants. Contextually, it is increasingly difficult to retrieve new mineral resources for the realization of building materials. Reusing ceramic industrial waste as precursors for building blocks/binders, exploiting their aluminosilicate composition for an alkaline activation process, could solve the problem. This chemical process facilitates the consolidation of new binders/blocks without thermal treatments and with less CO_2 emissions if compared with traditional cements/ceramics. The alkali-activated materials (AAMs) are today thought as the materials of the future, eco-sustainable and technically advanced. In this study, six different kind of industrial ceramic waste are compared in their chemical and mineralogical composition, together with their thermal behaviour, reactivity in an alkaline environment and surface area characteristics, with the aim of converting them from waste into new resources. Preliminary tests of AAM synthesis by using 80%–100% of ceramic waste as a precursor show promising results. Workability, porosity and mechanical strengths in particular are measured, showing as, notwithstanding the presence of carbonate components, consolidated materials are obtained, with similar results. The main factors which affect the characteristics of the synthetized AAMs are the precursors' granulometry, curing temperature and the proportions of the activating solutions.

Keywords: recycling; alkali-activated materials; ceramic; construction waste; geopolymers; sustainability

Citation: Fugazzotto, M.; Mazzoleni, P.; Lancellotti, I.; Camerini, R.; Ferrari, P.; Tiné, M.R.; Centauro, I.; Salvatici, T.; Barone, G. Industrial Ceramics: From Waste to New Resources for Eco-Sustainable Building Materials. *Minerals* **2023**, *13*, 815. https://doi.org/10.3390/min13060815

Academic Editors: Hendrik Gideon Brink, Pierfranco Lattanzi, Elisabetta Dore and Fabio Perlatti

Received: 4 May 2023
Revised: 3 June 2023
Accepted: 13 June 2023
Published: 15 June 2023

1. Introduction

Nowadays, the abundance of ceramic industrial waste constitutes an issue of global concern, and it requires a sustainable solution [1–3]. According to the current literature [4–7], about 45%–50% of the total construction and demolition (C&D) waste in the world is due to ceramic materials, while C&D waste in turn represents one third of the total waste generated by economic activities and households [8]. In particular, Italy produced 68 million tons of waste from construction and demolition before the pandemic event of the year 2020 [9]. Additionally, it should be considered that these official data are underestimated, since undesirable yet possible illegal dumping is not accounted for [8]. Besides the waste management problem, a further question arises, which must be faced urgently. Indeed, while the demand for construction materials grows [6,10,11], the availability of clay supply

in Italy and in other European countries is dramatically reduced [2,3,10]. As the most common of construction materials (cement, concrete, bricks, tiles, etc.) are obtained from clays, a consequent deep crisis in the entire field is obvious. In this scenario, the reuse of ceramic industrial waste as new feedstock for the production of building materials is attracting increasing interest, with the considerable advantage of minimizing the need to dispose of waste and exploit virgin clay deposits, as well as minimizing the negative environmental impact [1,3,12–15]. Due to their aluminosilicate composition and their partial amorphous phase, ceramics are cited among those waste materials which offer potential for valorization by alkali-activation [4,12,16,17]. Alkali-activated materials (AAMs) are hydraulic binders with amorphous structure and ceramic-like properties, chemically synthetized by the reaction between an alkaline solution and an aluminosilicate powder [18–21]. Consolidating at room temperature, or, at least, at much lower temperature compared to those required for making traditional cements or ceramics, the AAMs allow the abatement of CO_2 emissions. Furthermore, the use of ceramic waste supplied by local industries also promotes a process of circular economy [16]. As eco-sustainable materials, technically advanced and with performances similar to those of the traditional cements [18,19]—sometimes superior [22,23]—the AAMs could be considered the building materials of the future. Various studies have investigated the possibility to obtain AAMs from C&D waste [24,25], but the mix design, or formulation step, still remains challenging because of the heterogeneity of these products [14,26]. Undoubtedly, the use of construction debris is much easier than that of the demolition ones, because it is also easier to control their chemical and mineralogical composition [12]. However, the structure and the performance of AAMs strictly depend on the characteristics of aluminosilicate powders used as precursors [27–29]. Studying how different kinds of ceramics are alkali-activated is therefore important. An extensive experimental investigation was undertaken to compare six different kind of industrial ceramic waste (three kind of tiles, solid brick, hollow brick and stoneware) in terms of chemical and mineralogical composition, together with thermal behaviour, reactivity in an alkaline environment and surface area, with the aim of converting them from waste into new resources for the synthesis of alkali-activated products. Preliminary tests of synthesis, laboratory observations, compressive and porosimetric analysis are also performed. All the ceramic products selected are obtained from local clays and they are available in large quantities as waste, due to damage during the manufacturing process, decoration or during transport. They have therefore become unusable materials and, therefore, materials that need to be disposed of in landfills.

2. Materials and Methods

2.1. Materials

Different types of industrial ceramic wastes were selected as potential precursors for alkaline activation (Figure 1). Industrial and handmade tiles (labelled LBCa, LBCb, LBCc and LBCf) were provided by the local industry La Bottega Calatina, located in Caltagirone (CT), Italy; two types of red clay bricks (CWF and CWM) were recovered from the local industry Laquattro, located in Rometta (ME), Italy. All the ceramic products selected are pre-consumer waste.

LBCa is a tile waste characterized by a fine, homogeneous grain and pinkish body, made industrially by mixing commercial clay with 3% of water and fired at around 1100 °C, after natural drying. LBCb is a tile waste characterized by a coarse grain, dark red body, handmade by mixing local clay with a higher water percentage; volcanic aggregates and sand are present. The firing temperature to obtain it was between 900 and 1100 °C. LBCc is tile waste of medium grain size, semi-industrially produced, of reddish colour and homogeneous texture. LBCf is a stoneware tile waste, greyish in colour, perfectly homogeneous and smooth. LBCf was produced by an industrial process starting from kaolinitic clay fired at a temperature over 1300 °C. CWF is waste hollow brick, composed of ceramic materials fired at low temperature, around 870 °C, originating from local clay of the Plio-Pleistocene Rometta Formation retrieved from the areas of Fondachelli, San

Pier Niceto and Barcellona Pozzo di Gotto (Italy), and local sand aggregates. The texture is quite heterogeneous, light red in colour with fine grain size with white spots, probably of carbonate nature, and dark grains of millimetric size. Lastly, CWM is waste from solid brick, light red in colour, with a fine grain size and a homogenous texture. Sporadic silver/gold-like millimetric lamellae are visible together with some white spots. According to the literature [26,30–35], sodium hydroxide (NaOH) and sodium silicate (Na_2SiO_3) were selected as alkaline activating solutions. A concentration of 8 M NaOH was chosen in order to have an enough alkaline medium, preventing possible excessive efflorescence, without being excessively aggressive towards the environment. The desired molarity was obtained by diluting a commercial 10M NaOH solution, supplied by Carlo Erba, Milan (Italy). The sodium silicate used was provided by Ingessil srl, Verona (Italy); it is characterized by a module SiO_2/Na_2O = 3.3 and pH = 11.5. Metakaolin (MK), one of the main raw materials commonly used for the production of geopolymers because of its high reactivity [36–38], is used here in small amounts (maximum 20% of the solid precursor) in order to increase the reactivity and the performance of the ceramic-based geopolymers. The MK used is ARGICAL^{TM} M-1000, supplied by Imerys (France). Prompt (P), a natural cement prepared and supplied by Vicat Group (France), was also used as additive (in substitution of MK) in order to promote the reactivity of the ceramic precursors in the form of binary mixtures. It is commonly known as Roman cement and it is characterized by rapid setting (2–3 min) and hardening. The chemical composition of MK, according to the literature [36], and of P, according to the data sheet, are shown in Table 1.

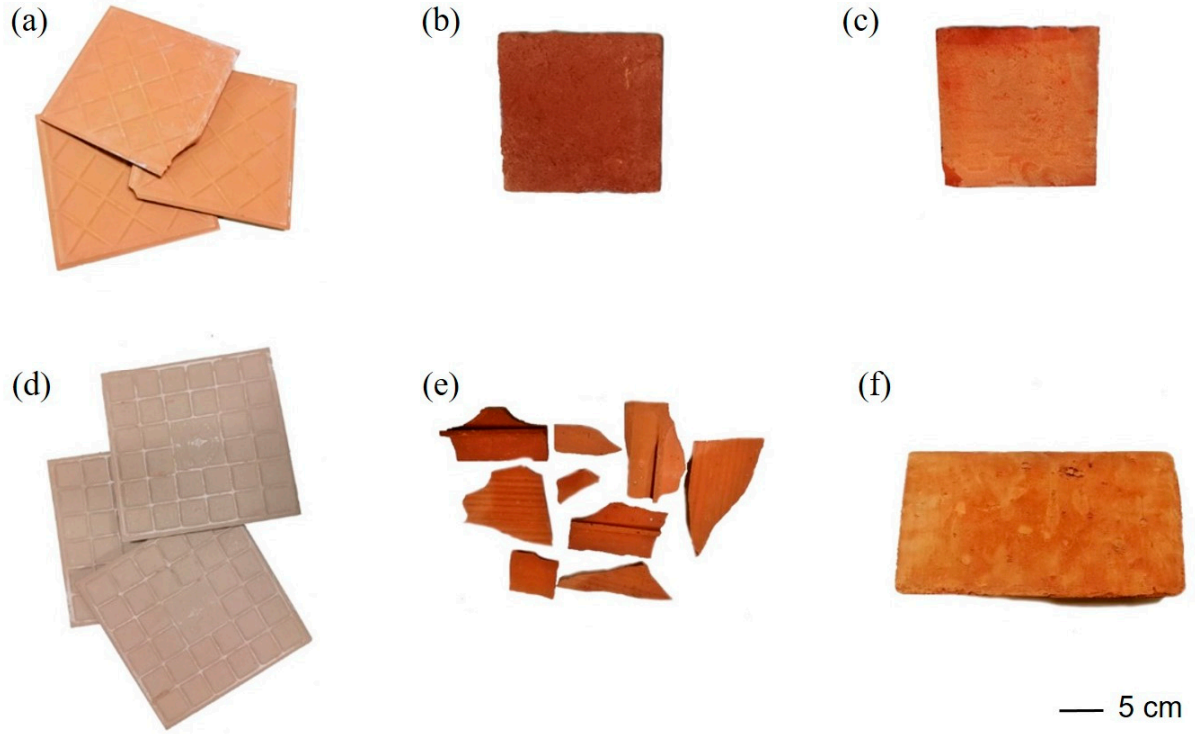

Figure 1. Ceramic waste retrieved by local industries: (**a**) LBCa; (**b**) LBCb; (**c**) LBCc; (**d**) LBCf; (**e**) CWF; and (**f**) CWM.

Table 1. XRF results on additives MK and P. nd = not determined.

Major Oxides (wt%)	SiO_2	Al_2O_3	Fe_2O_3	MgO	CaO	Na_2O	K_2O	TiO_2	P_2O_5	SO_3	LOI	Tot.
MK	58.56	34.03	2.57	-	2.08	-	0.69	1.88	0.2	-	nd	100
P	18.09	7.24	3.2	3.84	53.07	0.28	1.16	1.13	0.35	3.24	9.28	100

2.2. Synthesis Parameters

According to the suggestions of the producers, LBCa and CWF were selected for experimenting with alkali activation. Among all the ceramic waste supplied, indeed, these are the most abundant, and thus, those mainly responsible for the largest disposal problem. They are furthermore the most representative as industrial products and they are available in greater amounts for the tests. The synthesis process was carried out after preparing the solid and liquid raw materials. The LBCa and CWF raw materials were ground in porcelain jars with Al_2O_3 balls in order to reach the desired granulometry. The first tests were performed with a LBCa ground to around 75 µm. A granulometry similar to that of commercial MK was also chosen (~10 µm). For experimenting with binary mixture, MK or P were dried in an oven and sieved before adding them, separately, to the ceramic powders, in order to avoid the formation of agglomerates. The powdered components were carefully homogenized in a porcelain jar before the addition of the activating solution. Preliminary tests using only sodium hydroxide yielded poor results in setting and curing of the pastes. Thus, alkali-activated mixtures of sodium hydroxide and sodium silicate were tested, as well as activation by using only sodium silicate. When a mixture of sodium hydroxide and sodium silicate was used, it was allowed to rest for some minutes before the synthesis, in order to avoid the effect of the exothermic reaction between the two liquids on the geopolymerization [39,40]. The liquid was then poured on the powders, and immediately subjected to mechanical mixing for 5 min. The so-obtained slurries were then poured into molds and manually agitated for 1 min in order to facilitate the escape of air bubbles from the mixture [8,26,33]. After 24 h at room temperature, the samples were demolded and wrapped with polyethylene film for the remaining curing time (fixed at 28 days). Maturation was carried out at room temperature, around 25 °C, avoiding firing procedures in order to reduce environmental impact. However, some formulation replicates were also subjected to a low-temperature treatment (65 °C) for the first 24 h after synthesis [41], in order to assess the effect of different curing temperatures. The best liquid/solid (L/S) ratio for each formulation was defined according to the workability of the slurry during the synthesis, while also considering the setting and curing times.

2.3. Analytical Methods

The as-received industrial ceramic wastes were characterized by X-ray Fluorescence (XRF), X-ray Diffractometry (XRD), Reactivity Test + Inductively Coupled Plasma—Optical Emission Spectroscopy (ICP-OES) and Thermogravimetric Analysis (TGA). The ground samples were characterized via laser granulometry and Brunauer–Emmett–Teller analysis (BET), while the obtained geopolymeric samples were studied using integrity tests, visual critical evaluations and tested by Mercury Intrusion Porosimetry (MIP) and uniaxial compressive test. Where present, the efflorescence was investigated by XRD. Chemical analyses by XRF were performed on pearls by a PANalytical instrument, model Zetium, with ceramic tube with Rh anode; ultra-fine high transmission Beryllium front window, at least 75 µm and tube geometry below the sample; High Stability Power 4 kW X-ray Generator; decoupled goniometer θ/2θ with optical positioning system and high angular reproducibility (0.0001°) (CIC—University of Granada, Spain). Mineralogical investigations were performed by a PANalytical X'Pert PRO X-ray Diffractometer, with Cu Kα radiation and operating at 45 kV and 40 mA; the following operative conditions were used: time 20 s, step 0.04 in a range of 3–70 2θ (Department of Mineralogy and Petrology—University of Granada, Spain). The qualitative analysis was then conducted by using High Score Plus software v.4.8. The reactivity test was performed following the experiments according to the literature [42,43]; however, while they usually use HF, in this research the tests were carried out reproducing the solubility conditions chosen for the alkaline activating process, namely, ambient T and pH of a NaOH 8 M solution. An amount of 1 ± 0.05 g powder of each material was subjected to a reactivity attack by using NaOH 8 M (NaOH, 99%, J. T. Baker; water Millipore purified by Milli-Q UV, resistivity > 18 MΩ·cm) in 100 mL of solution. The system was mechanically agitated (300 rpm) for 12 h at room temperature. The

analysis of the eluate allowed the determination of the solid residue using the gravimetric method, and obtained the amount of soluble Si and Al by ICP-OES. In particular, after the basic attack, the eluates were filtered with Whatman paper and diluted with Milli-Q water until reaching the volume of 1 L. The washing of the filters was carried out until reaching a neutral pH. The solid residues were then obtained after drying in an oven at 110 °C for 1 h. A Varian 720-ES ICP—OES was used for the chemical analysis of the eluates by introducing the sample via a spray chamber. The quantification was obtained by using the internal standard method of Ge (1 mg/L); the calibration curve was realized considering 6 points in the 2–200 µg/L interval (CSGI and Department of Chemistry—University of Florence, Italy). TGA was performed by using a thermobalance TA Instrument, model Q5000IR, according to the procedure reported in [44,45]. The analyses were performed on about 10–15 mg of sample in a nitrogen flux, with gradual increases of 20 °C/minute, considering a temperature range from the environmental temperature to a maximum of 900 °C (Department of Chemistry and Industrial Chemistry—University of Pisa, Italy). Granulometric measurements were carried out by using the Laser Granulometer Mastersizer 2000, Hydro 2000S model (Malvern Instrument). The measurements were conducted in humid conditions; after the acquisition of a "white" reference, 10 successive acquisitions for each sample were elaborated by the software, which returned an average curve. The results were then expressed with a cumulative curve and a curve representing the granulometric distribution. BET analyses were performed by using the Micromeritics Instrument, Gemini Model 2380, with the following technical specifications: N_2 analysis adsorptive, 10 s equilibration time and pressure of 1.03979×10^5 Pascal (Department of Engineering "Enzo Ferrari"—University of Modena and Reggio Emilia, Italy). Preliminary evaluations of the pastes were conducted by simple observation of a few criteria concerning the curing time required to demold the geopolymers, their complete hardening (when the surfaces are completely dry), the tendency to shrink, the appearance in terms of homogeneity and the efflorescence crystallization. The integrity test, on the other hand, is a preliminary test generally adopted by the scientific community working with AAMs in order to check the stability of the material in water, when soaked for 24 h [39]. The integrity test could be, thus, considered a first step in the evaluation of the advancement of the geopolymerization process, i.e., the formation of the alkaline gel [39]. The visible parameters considered to check the sample's integrity were the appearance of water (clear, with residues, turbid) and the tendency of the geopolymeric fragment to be broken by a metallic pincer with hand pressure. A formulation passes the test if the water remains clear and the geopolymer does not break with the pincer (Figure 2).

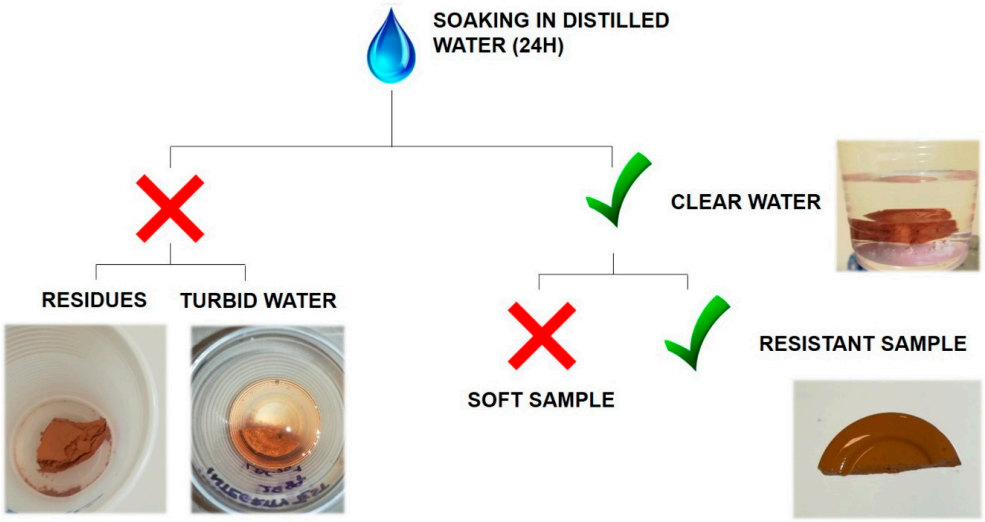

Figure 2. Integrity test scheme.

Three samples of 2 × 2 × 2 cm^3 for preliminary compressive tests were analysed by the Instron Model 5592 instrumentation, maximum charge of 600 kN and a velocity of 0.5 MPa/s, according to CEN EN 1926:2006 standard [46] (Department of Earth Science—University of Florence, Italy). For MIP, a Thermoquest Pascal 240 porosimeter was used in order to explore the pore size distribution with radii between 0.0074 mm and 15 mm, and a Thermoquest Pascal 140 porosimeter to investigate the pore radii range 3.8 mm–116 mm (Department of Biological, Geological and Environmental Sciences—University of Catania, Italy). Before the analysis, the fragments were dried in an oven for 24 h at 100 °C.

3. Results and Discussion

3.1. Chemical Composition of the Ceramic Industrial Wastes

The XRF results are shown in Table 2. Data related to LBCa major oxides are reported from the literature [16].

Table 2. XRF results on the ceramic waste materials selected as precursors.

Major Oxides (wt%)	SiO_2	Al_2O_3	Fe_2O_3	MnO	MgO	CaO	Na_2O	K_2O	TiO_2	P_2O_5	Others	LOI	Tot.
LBCa	60.67	16.30	5.69	0.08	2.31	8.73	1.35	3.27	0.69	0.14	0.30	0.47	100
LBCb	57.91	17.33	7.53	0.11	2.58	7.41	2.35	2.30	1.13	0.35	0.53	0.47	100
LBCc	61.17	17.03	5.63	0.04	2.08	7.81	0.49	4.02	0.76	0.17	0.29	0.51	100
LBCf	72.37	18.37	0.99	0.01	0.54	0.80	3.22	2.37	0.68	0.12	0.18	0.35	100
CWF	57.33	14.32	5.51	0.08	2.43	11.99	1.16	2.49	0.73	0.17	0.33	3.46	100
CWM	56.83	15.20	5.63	0.07	2.52	10.15	1.39	2.80	0.70	0.18	0.21	4.32	100

The materials show similar chemistry, with the exception of sample LBCf. In general, all the materials show a SiO_2 content between 57 and 61 wt%. The second important chemical component is Al_2O_3, with values between 14 and 18 wt%. CaO is the third component of the chemistry, with values between 7 and 12 wt%. Another important element is Fe_2O_3 (more than 5 wt%). The LBCf sample is the exception, showing the highest values of silica reaching 72 wt%, while it could be considered free of calcium and iron components. All the materials show a different LOI%, with very low values for the LBC samples and higher values for CWF and CWM, which suggests the presence of carbonate phases in these latter samples due to the lower firing temperature of bricks. This is confirmed below by XRD analysis. In this context, the relatively high CaO content of the LBC samples is attributable to non-carbonate phases, as calcium-rich silicates. The amounts of the three major oxides, SiO_2%, Al_2O_3% and CaO% are plotted in the triangular diagram (Figure 3), showing the usual range of the composition of the aluminosilicate materials most commonly used as precursors in the field of AAMs, and OPC as comparison—sketched approximately according to [20]. It is evident that the ceramic waste has an intermediate composition, with a high percentages of silica in comparison to the other materials, somewhat less alumina and an intermediate content of CaO. Relative to this component, the studied ceramic wastes are placed between the materials known as "low-calcium" (as metakaolin and fly ash) and those of "high calcium" (as blast furnace slag) [20]. Particularly, they are located near the limit area of fly ash, with a higher silica content. LBCf, on the other hand, falls much closer to the SiO_2-Al_2O_3 axis, because of the absence of the CaO component. The data are consistent with further studies on the composition of aluminosilicate materials used for making AAMs [47].

3.2. Mineralogical Composition of the Ceramic Industrial Wastes

The individuated phases for each sample are shown in Table 3, where the data related to LBCa come from the literature [16]. Mineral abbreviations are reported as in [48]. As expected from the XRF data, LBC samples are distinguished from the CWF-CWM samples because of the absence of calcite and muscovite/illite, which instead characterize the

latter. Quartz, feldspars and haematite are present everywhere, while diopside, gehlenite, wollastonite and montmorillonite differentiate the mineralogical compositions of the LBC samples among themselves. Furthermore, the results for LBCf, being a different kind of ceramic product, are very different. It is composed almost completely of quartz, feldspars and mullite. It is the only sample where haematite is not present.

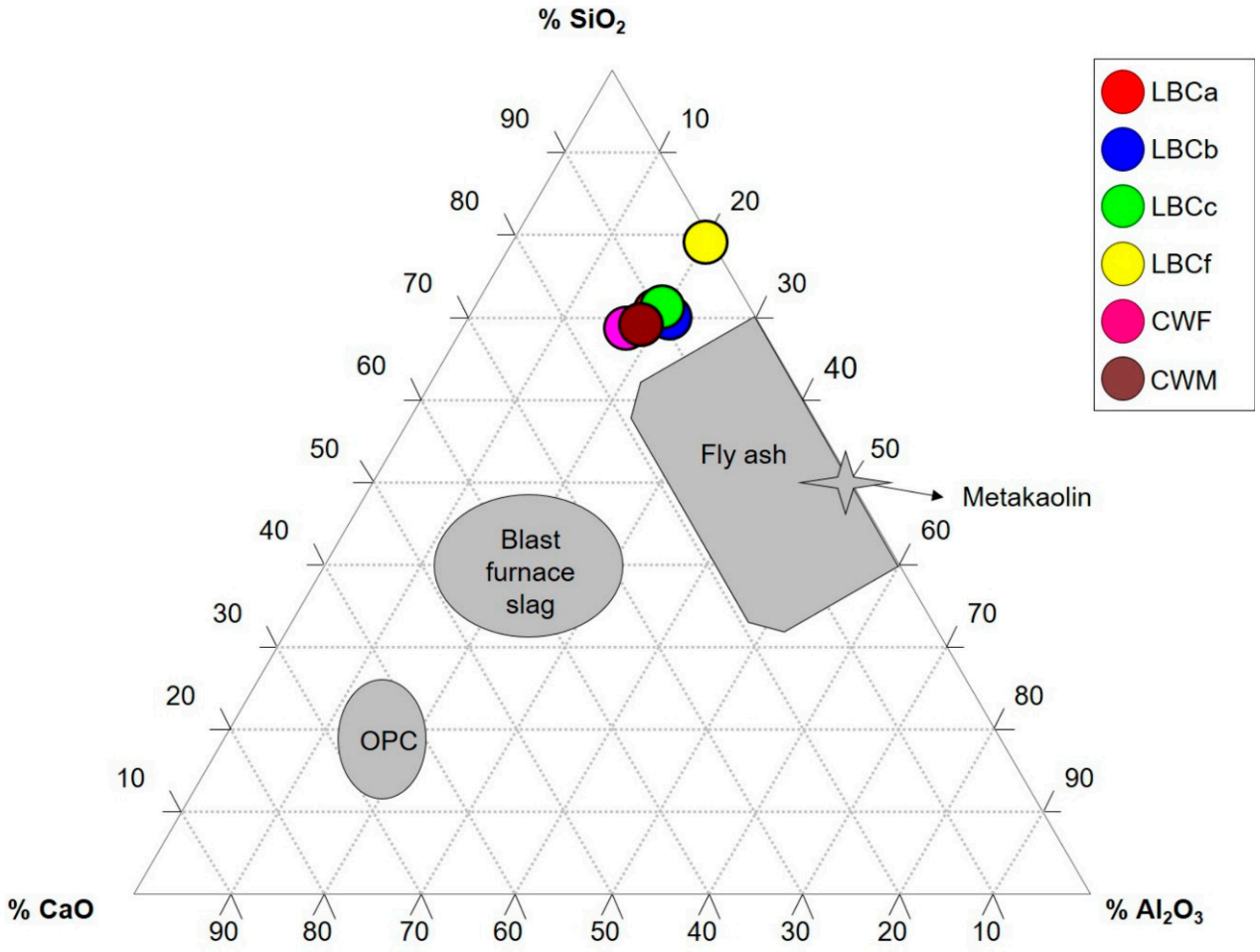

Figure 3. Triangular diagram CaO-SiO_2-Al_2O_3 for the ceramic waste composition. The colored circles represent the ceramic waste analyzed, while the grey areas indicate the compositional range of typical raw materials used for geopolymerization. The compositional range of typical OPC is also marked on the diagram.

Table 3. Mineralogical phases detected on ceramic waste samples; Qz = quartz, Fsp = feldspar, Hem = hematite, Di = diopside, Gh = gehlenite, Wo = wollastonite, Mnt = montmorillonite, Cal = calcite, Ms = muscovite, and Mul = mullite; X = present, / = absent.

Sample	Qz	Fsp	Hem	Di	Gh	Wo	Mnt	Cal	Ms	Mul
LBCa	X	X	X	X	X	X	/	/	/	/
LBCb	X	X	X	X	/	/	X	/	/	/
LBCc	X	X	X	X	X	/	/	/	/	/
LBCf	X	X	/	/	/	/	/	/	/	X
CWF	X	X	X	X	X	/	/	X	X	/
CWM	X	X	X	/	/	/	/	X	X	/

3.3. Thermogravimetric Behavior of the Ceramic Industrial Waste

From the TG curves reported in Figure 4 and the values of Table 4, it is possible to distinguish two groups corresponding to the observed groups of the LOI%. A high mass loss residue is registered, about 99% at 850–900 °C for the LBC samples, while relatively lower values are observed for the CWF and CWM samples, respectively, of 97% and 95.8%. It is possible to note how the two groups are characterized by different patterns of mass loss. Apart from the mass loss occurring in the temperature interval 80–200 °C, attributed to surface or hygroscopic water loss, several steps attributable to the dehydroxylation of clay minerals are visible in the LBC samples. The CWF and CWM TG curves are dominated by the step at 600–900 °C, typical of a decarbonation process, attributable to the calcite already detected by XRD and LOI%.

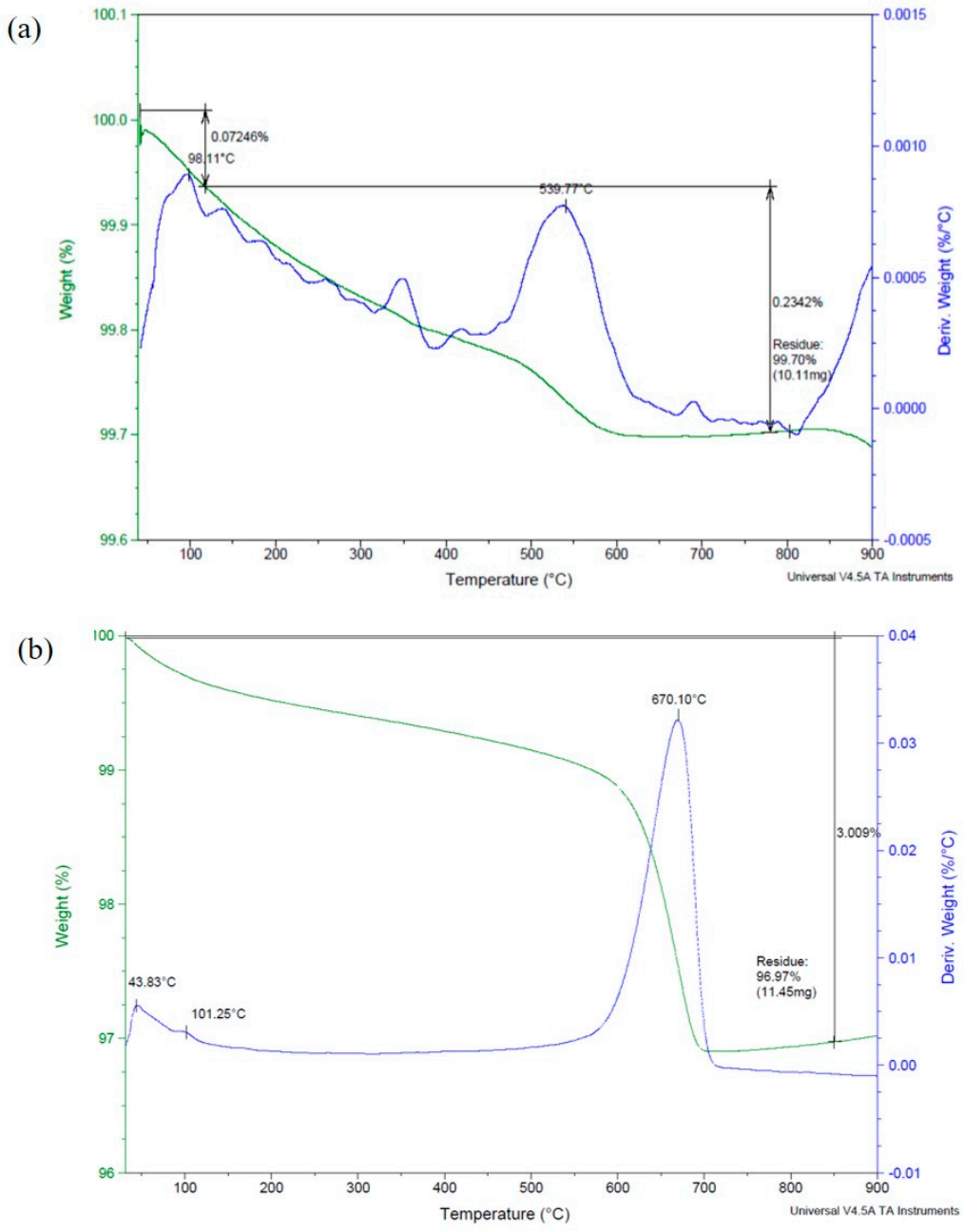

Figure 4. TG curves of two representative ceramic waste materials: (**a**) LBCa, representative of the tiles group LBC; and (**b**) CWF, representative of the bricks group CWF-CWM.

Table 4. Decomposition temperatures and mass loss of the ceramic industrial wastes under study. Residual mass at 850 °C.

Sample	0–80 °C	80–130 °C	130–200 °C	200–500 °C	500–600 °C	600–900 °C	Residue (%)
LBCa		0.15		0.05	0.09		99.7
LBCb		0.14			0.19		99.7
LBCc			0.4				99.6
LBCf	0.12			0.4			99.5
CWF *	0.36					2.7	97
CWM *	0.78	0.24				3.2	95.8

* Data partially reported from the literature [45].

3.4. Reactivity Test in Alkali of Ceramic Industrial Waste

As it is well known, the total amount of silica and alumina present in a ceramic material could not be considered reactive [20,49]. In order to investigate how much of these components are potentially reactive in alkaline media [20], a reactivity test was performed on all the ceramic industrial waste, evaluating their solubility in 8 M NaOH solution at room temperature, and the obtained solution was analysed by ICP-OES. LBCb was analysed as representative of the group of handmade tiles LBCb-LBCc. By the gravimetric measurement of the solid residue, the soluble phase (that means potentially reactive) was obtained (Table 5). The sample with the highest value of soluble phase was CWM, with 30 wt% of soluble phase, while LBCa and CWF showed the lowest value of soluble phases, respectively, with a solid residue of 90 and 94 wt%.

Table 5. Data results of ICP-OES on the eluates after reactivity test on ceramic waste: solid residue (wt%), soluble fraction (wt%), analytical results of the Si and Al concentration (mg/L) and comparison between the Si and Al amount solubilized with the reactivity test and the soluble fraction (% as solid completion).

Sample	Solid Residue (wt%)	Soluble Fraction (wt%)	Si (mg/L)	Al (mg/L)	Si + Al (mg/L)	(Si + Al)/Soluble Fraction (wt%)
LBCa	90	10	9.5	3.1	12.63	12
LBCb	84	16	8.1	3	11.07	7
LBCf	83	17	15.7	3.8	19.48	11
CWF	94	6	10	3.6	13.61	22
CWM	70	30	22.1	14.6	36.7	12

Table 5 also shows the Si and Al concentrations of the eluates determined by the ICP-OES. As expected, the solubility results were higher for Si than for Al. The contribution sum of Si and Al and their percentage in the soluble phase brings to light the highest value calculated for CWF. The high percentage of solid residue after NaOH treatment was observed in the literature. Different studies indeed demonstrated that the alkali attack, even performed under different conditions of sodium hydroxide concentration, temperature or treatment time, give only a partial dissolution of the Si and Al of the aluminosilicate material [50–52]. Their soluble fraction in alkaline solution is also linked to the nature of the aluminosilicate materials; for example, it seems that tectosilicates are more sensitive to this kind of treatment than phyllosilicates, inosilicates or cyclosilicates [50]. Furthermore, the ability of the aluminosilicate material to exchange cations, the Al^{3+} coordination and the surface area influence the Si and Al dissolution [51,52]. In order to understand the percentage of potentially reactive silica and alumina, the obtained results were recalculated on the total silica and alumina amount measured from the bulk chemical composition of the ceramic precursors. The final data are shown in Table 6.

Table 6. Amount of silica and alumina dissolved after basic attack, calculated on the total silica and alumina amount measured from the bulk chemical composition of ceramic precursors tested. SiO_2% s Tot = soluble SiO_2% with respect to the total chemical composition of the sample; Al_2O_3% s Tot = soluble Al_2O_3% with respect to the total chemical composition of the sample; SiO_2% s Silica Tot = soluble SiO_2% with respect to the total SiO_2% present in the sample; Al_2O_3% s Alumina Tot = soluble Al_2O_3% with respect to the total Al_2O_3% present in the sample.

Sample	SiO_2% s Tot	Al_2O_3% s Tot	SiO_2% s Silica Tot	Al_2O_3% s Alumina Tot	$[SiO_2]/[Al_2O_3]_{reactive}$
LBCa	0.002	0.001	0.328	0.359	3.397
LBCb	0.002	0.001	0.299	0.327	3.057
LBCf	0.003	0.001	0.464	0.391	4.678
CWF	0.002	0.001	0.373	0.475	3.145
CWM	0.005	0.003	0.832	1.815	1.714

The amount of the soluble silica and alumina of the ceramic precursors under these conditions (NaOH 8M solution at room temperature) is very low, less than 1% of the total silica and alumina detected by XRF. Only the CWM sample is an exception, with a value of around 2%. The low measured value could be highly affected by the reprecipitation of SiO_2 and Al_2O_3 as, for instance, sodium silicates and aluminates. Nevertheless, the $([SiO_2]/[Al_2O_3])_{reactive}$ ratio of the studied ceramic industrial wastes is on average around 3. This is considered a critical parameter, which in order to obtain a good mechanical performance in geopolymers, should be between 2 and 4 [20]. Only the CWM sample is quite below the threshold.

3.5. Granulometric Analysis on Ceramic Waste (Laser Granulometry and BET)

As preliminary synthesis tests were performed using LBCa and CWF as raw materials, a granulometric investigation was performed on these two ceramic wastes. While preliminary tests were performed with a granulometry of 75 µm, a lower granulometry, at least 15 µm, was preferred for the larger synthesis set. Starting from centimetre-sized fragments of ceramics (1–2 cm), different grinding procedures were tested in order to reach the desired granulometry. The preferred individuated procedure consisted of 40 min grinding in a porcelain jar with alumina spheres, in accordance with the literature [41]. About 50% by volume of the particles had a size of about 16 µm and 12 µm, measured by laser diffraction, obtained for LBCa and CWF ceramics, respectively (Figure 5).

As is immediately visible, furthermore, the LBCa particle size distribution shows a unimodal pattern, with a mean particle size of around 10 µm, while CWF is characterized by a bimodal particle size distribution, with mean particle sizes around 1 µm and 10 µm. The obtained powder fineness is similar to that of Portland cement, having particles in the size range 1–100 µm [35], and to that of MK, which was also used in this research project. During material processing, its specific surface could change; thus, BET analyses were performed in order to evaluate the correlation between the granulometric analysis and the superficial area [53]. It was found that when the granulometry decreases, the specific area of the LBCa ceramic increases, while that of CWF decreases (Table 7), even if there is a significant difference between the sintered ceramic product fired at 1100 °C compared to porous bricks fired under 1000 °C.

3.6. Visual Observations and Integrity Tests

Around fifty formulations were synthesized and, after 28 days of curing, submitted to preliminary considerations and to the integrity test. In the Supplementary Materials (Table S1), all the formulations and their synthesis parameters are shown. Table 8, on the other hand, summarizes the preliminary evaluations and the results of the integrity tests.

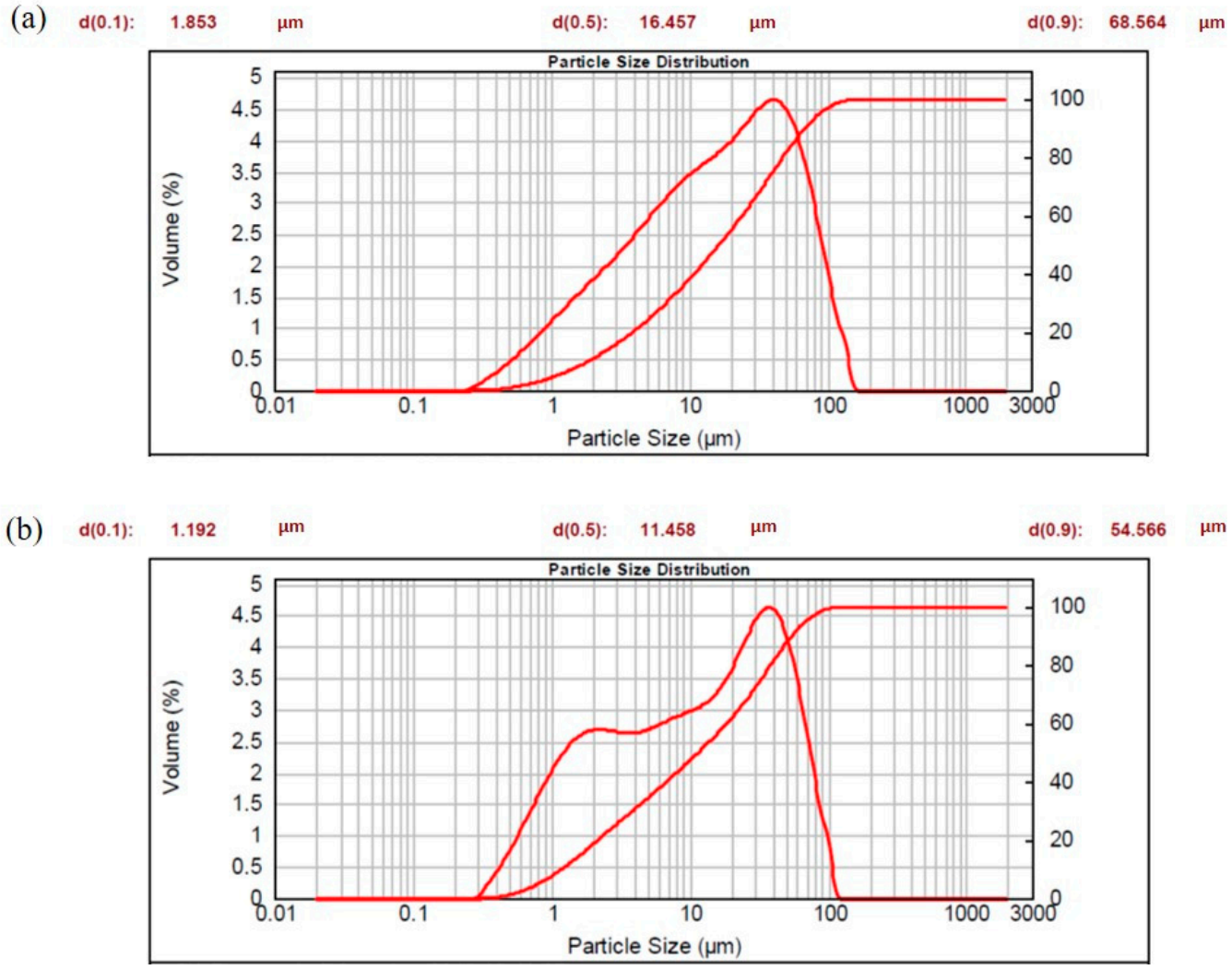

Figure 5. (**a**) Particle size distributions of LBCa; and (**b**) particle size distributions of CWF; measured by laser granulometry. d(0.5) = 50% of volume with the particle size less than this dimension; and d(0.9) = 90% of volume with the particle size less than this dimension.

Table 7. BET analysis results of the selected precursors.

Sample	D_{50}	Surface Area (m^2/g)
LBCa	1–2 mm	0.5272
	~15 µm	1.0155
CWF	>125 µm	47.8880
	~12 µm	43.1090

Table 8. Preliminary observations and integrity test results of the experimental AAMs: St = setting time and Ct = curing time.

Sample	St (min)	Ct (Days)	Homogeneity	Shrinkage	Cracks	Salts	Integrity Tests	
							Stability in Water	Resistance to Pincer
$LBCa_{75}$ 1	/	28	no	yes	no	no	no	no
$LBCa_{75}$ 2	/	28	no	yes	no	no	no	no
$LBCa_{75}$ 3+50P	/	28	yes	yes	no	no	yes	no
$LBCa_{75}$ 4	/	28	no	yes	no	no	no	no

Table 8. *Cont.*

Sample	St (min)	Ct (Days)	Homogeneity	Shrinkage	Cracks	Salts	Integrity Tests	
							Stability in Water	Resistance to Pincer
$LBCa_{10}$ 1	5	28	yes	yes	no	no	no	no
$LBCa_{10}$ 2	5	28	yes	yes	no	no	no	no
$LBCa_{10}$ 3+50P	5	1	yes	yes	no	no	yes	no
$LBCa_{10}$ 4	5	28	no	yes	no	no	no	no
LBCa 5	5	1	no	yes	no	no	no	no
LBCa 5A	5	1	no	yes	no	yes	yes	no
LBCa 5+10MK	5	1	yes	yes	no	no	yes	no
LBCa 5+10MK_A	5	1	no	yes	no	yes	yes	no
LBCa 5+20MK	5	1	yes	yes	no	no	yes	no
LBCa 6	5	1	yes	yes	no	no	no	no
LBCa 6+10MK	5	1	no	yes	no	no	no	no
LBCa 6+20MK	5	1	yes	yes	no	no	no	no
LBCa 7	5	1	yes	yes	no	no	no	no
LBCa 8	5	1	yes	yes	no	no	no	no
LBCa 9	5	7	yes	yes	no	no	no	no
LBCa 10	5	7	yes	yes	no	no	no	no
LBCa 11	5	1	no	yes	no	no	yes	no
LBCa 12	5	1	yes	yes	no	yes	yes	no
LBCa 12A	5	1	yes	yes	no	yes	yes	no
LBCa 13	5	7	yes	yes	no	no	yes	yes
LBCa 13+10MK	5	1	yes	yes	no	yes	yes	yes
LBCa 13+20MK	5	1	yes	no	no	no	yes	yes
LBCa 14	5	7	yes	yes	no	no	yes	yes
LBCa 14+10MK	5	1	yes	yes	no	no	yes	yes
LBCa 14+20MK	5	1	yes	no	no	no	yes	yes
LBCa 14+5P	5	<1	yes	yes	no	no	yes	yes
LBCa 14+10P	2	<1	yes	yes	no	no	yes	yes
LBCa 14+20P	2	<1	yes	yes	no	no	yes	yes
LBCa 15	5	7	yes	yes	no	yes	yes	no
LBCa 15+10MK	5	1	yes	yes	no	yes	yes	yes
LBCa 15+20MK	5	1	yes	no	no	yes	yes	yes
CWF 13	5	7	yes	yes	no	no	yes	yes
CWF 13+10MK	5	1	yes	yes	no	no	yes	yes
CWF 13+20MK	5	1	no	no	no	no	yes	yes
CWF 14	5	7	yes	yes	no	no	yes	yes
CWF 14+10MK	5	1	yes	yes	no	no	yes	yes
CWF 14+20 MK	5	1	yes	no	no	no	yes	yes
CWF 15	5	7	yes	yes	no	yes	no	yes
CWF 15+10MK	5	1	yes	yes	no	yes	no	yes
CWF 15+20MK	5	1	yes	no	no	yes	no	yes

The first observation is the failure of the formulations made with 75 µm powders, which do not set, but harden just because of drying after very long times. Indeed, they totally failed the integrity tests, with the exception of the sample with 50% of P. The setting time was then accelerated to 5 min by the decrease in the granulometry of the ceramic precursor. As reported in the literature [54], indeed, the powders' reactivity is also determined by its fineness, increasing with the decrease in the granulometry. The curing time instead ranges from 1 to 7 days, likely depending on the liquid content of the fresh paste and on the degree of reactivity of the ceramic industrial waste [34,55]. The majority of the samples show a fairly homogeneous visual appearance, with some exceptions probably due to insufficient mixing of the different components in binary mixtures, or due to a separation of the sodium silicate, which tends to stratify at the top of the poured samples, when in excess. In some cases, the lack of workability observed during the synthesis makes the surface of the dried samples rough because of an increased difficulty in pouring the slurry into the mold. The tendency to shrink characterizes all the samples, with the exception of those with the highest amount of MK. Nevertheless, the extent of the shrinkage upon drying could be considered low, as it did not produce any cracks nor micro-cracks, and it should be considered as an intrinsic characteristic of this kind of material [56]. In order to reduce drying shrinkage in the final products, inert aggregates should be

added in the mix design [57]. Regarding the efflorescence, it is evident that this appears when the sodium hydroxide proportion in the liquid component is higher (e.g., sodium hydroxide/sodium silicate = 2.33), or when moderate amounts of sodium hydroxide (e.g., sodium hydroxide/sodium silicate ~ 0.5) is combined with high amounts of water added during the synthesis. Furthermore, efflorescence appears in samples which were subjected to a low-temperature firing step, probably because of the faster evaporation of water compared to the replicates cured entirely at room temperature [26,27,33]. Regarding the stability in water and the resistance to the pincer cut after soaking, it is possible to see in Table 8 how the first synthesis tests totally failed both criteria of the integrity test, with the exception of the fired samples and of the binary mixtures. The apparent quick setting and apparent consolidation of all the samples which tend to disintegrate in water could probably be ascribed to the hardening action of the drying of sodium silicate [26,40,58], generally present in high amounts, without the occurrence of an efficient geopolymerization process. In the second part of the table, the results of the integrity tests show samples leaving the water clear and resisting the pincer cut. Among these, the formulations obtained by adding a percentage of P are characterized by a very quick setting time, which is a very promising result for the scale-up of building materials. After considering the preliminary results of the empirically adjusted slurries in the lab, a batch of LBCa-based formulations (highlighted in grey in Table 8) was selected to be replicated using CWF as a precursor. The last lines of Table 8 show that by changing the ceramic precursor, similar results are obtained in terms of preliminary visual observation and the results of the integrity test.

3.7. Mechanical Resistance and Porosity of Alkali-Activated Samples

The formulations tested both with curing at room temperature and with a 65 °C treatment were analyzed. Uniaxial compressive tests and mercury porosimetry were performed in order to investigate the effect of the curing temperature step on the performance of the final hardened product. The results are summarized in the scheme of Figure 6, and shown in detail in the Supplementary Materials (Tables S2 and S3).

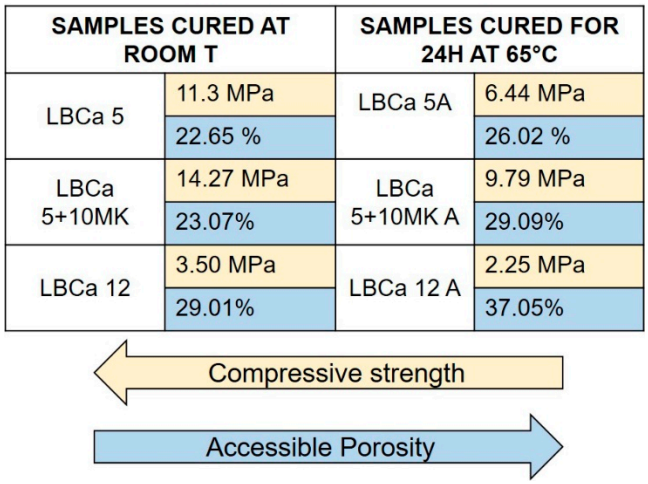

Figure 6. Porosimetric and mechanical results obtained from samples LBCa 5, LBCa 5+10MK and LBCa 12, cured at ambient temperature, and on the corresponding samples cured for 24 h at 65 °C and then allowed to mature at room temperature: LBCa 5A, LBCa 5+10MK_A and LBCa 12A.

The samples LBCa 5 and LBCa 5+10MK do not show visible efflorescence, while the same formulations after the firing step (LBCa 5A and LBCa 5+10MK_A) are characterized by visible efflorescence as well as a decrease in compressive strength of about 5 MPa. The simultaneous occurrence of these features could be correlated to the same event, i.e., the crystallization of crypto-efflorescence would interrupt the structural continuity of the alkaline gel in the samples, compromising their compactness and resistance [59]. Decreases in compressive strength are also individuated in LBCa 12A (same formulation as LBCa 12,

but cured at 65 °C), but in this case efflorescence is already visible in the non-fired sample. In general, the resistance of both samples is very poor, while the strength value for the other samples could be considered within the range of other AAMs [60]. Concerning porosity, the samples show values of accessible porosity between those of traditional cement and typical geopolymers [61]. It is furthermore possible to notice an increase in the accessible porosity after firing, which is an inverse pattern with respect to that observed for the compressive strength values. Again, the fired samples show worse performances than those cured at room temperature. The higher accessible porosity volume would indeed determine a higher vulnerability of the products to environmental decay. From the results shown in Figure 6, it is furthermore possible to appreciate how the addition of only 10% of MK to the solid precursor determines an increase in the compressive strength of the final product.

3.8. Mineralogical Investigation of the Efflorescence

In order to investigate the efflorescence formed on the samples, a few samplings were carried out on the powdery deposit of salts when present; otherwise, the salt samples were scratched from the surface with a scalpel. In this latter case, we must consider the possibility that the geopolymer was sampled as well. XRD was carried out on samples LBCa 12A, LBCa 13+10MK, LBCa 15, LBCa 15+10MK and LBCa 15+20MK. The diffraction pattern of salts collected from sample LBCa 15+20MK is shown in Figure 7 as representative. From this analysis, mainly sodium carbonates with different hydration grades were detected, as expected [62–64]. Some further peaks cannot be attributed to sodium carbonates, and are mainly compatible with the presence of gypsum; however, its presence cannot be confirmed by XRF analysis, since sulfur was not revealed. In detail, trona ($Na_3(CO_3)(HCO_3)$*$2(H_2O)$) and thermonatrite ($Na_2CO_3(H_2O)$) were individuated in sample LBCa 15, in samples LBCa 13+10MK and LBCa 15+20MK (with the possible presence of gypsum ($CaSO_4$*$2H_2O$)) and in sample LBCa 12A (with the possible presence of ettringite ($Ca_6Al_2(SO_4)_3(OH)_{12}$*$26(H_2O)$); only thermonatrite was detected in sample LBCa 15+10MK. In some samples, peaks attributable to quartz, most likely due to the geopolymeric substrate scratched unintentionally during sampling, are also present.

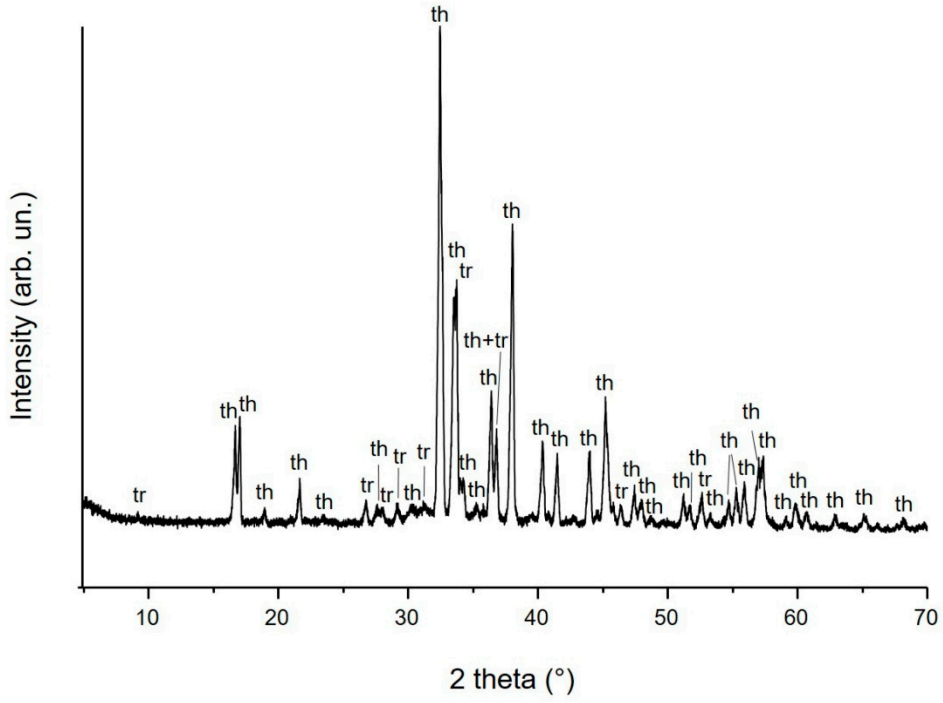

Figure 7. Representative diffraction pattern of the salts collected from the samples LBCa 12A, LBCa 13+10MK, LBCa 15, LBCa 15+10MK and LBCa 15+20MK. The diffraction pattern of the sample LBCa 15+20MK in particular is shown in the image. th = thermonatrite; tr = trona.

4. Conclusions

Six different industrial waste samples of ceramic materials were analyzed to determine their chemistry and mineralogy, thermal behavior, and reactivity in the alkaline environment required for the synthesis of AAMs. On two selected ceramic wastes, selected according to their representativeness and higher abundance in the industries, the effect of particle size on the properties of the final products was investigated. A plethora of formulations were designed and prepared from the same kind of ceramic by varying the type of alkaline solutions, L/S ratio, amount and kind of additives, and curing conditions. A set of formulations were replicated by changing the waste used as an aluminosilicate precursor. Visual observations of fresh samples were recorded during the synthesis, and preliminary tests were carried out after 28 days. The main important conclusions can be summarized as follows:

- The comparison of performances among the ceramic wastes distinguished two groups related to the presence or absence of calcite. This demonstrates, as we could expect, a different behavior at high temperatures and in alkaline conditions. Nevertheless, by using two ceramics representative of the two individuated groups (LBCa and CWF) for the synthesis, similar results were obtained in terms of workability, curing time, possible efflorescence formations, cracks or shrinkage and water resistance (integrity tests);
- The results obtained reveal that construction industrial wastes of ceramic nature can be activated by using proportioned mixtures of sodium hydroxide (8 M) and sodium silicate (R = 3.3), in accordance with the literature [61], or with only sodium silicate;
- AAMs tend to consolidate between 1 day and 7 days, depending on the formulation and particularly on the amount of additives;
- P and MK, even if added in small amounts (5%–10%), are able to promote the alkaline gel building, and thus the consolidation. Such additives also improve the strength and counteract the formation of efflorescence;
- Where present, the efflorescence seems to be strictly linked to the higher sodium hydroxide or water amount; therefore, as well as with the addition of additives, the formation of efflorescence could be avoided by balancing formulations in a stoichiometric way;
- In contrast to the current literature [4,26,65], this study highlighted that curing at room temperature (around 25 °C) is preferable, whereas thermal curing at 65 °C for 24 h resulted in lower performance in terms of compressive strength and an increase in porosity, and facilitated efflorescence crystallization. Similar results were also found in [39];
- LBCa and CWF proved to be the least reactive ceramics among all the samples studied. Despite that, good results for the synthesis of AAMs were obtained, allowing for better results by using the other, more reactive, ceramic wastes characterized here.

Supplementary Materials: The following supporting information can be downloaded at https://www.mdpi.com/article/10.3390/min13060815/s1. Table S1: Synthesis parameters of AAMs experimented: *the % is calculated on total solid; **the % is calculated on total liquid; Tc = curing temperature; Table S2: Results of uniaxial compressive strength tests performed on examples of geopolymers cured at room temperature and at 65 °C for 24 h; Table S3: Porosimetric data of geopolymeric examples cured at room temperature and at 65 °C for 24 h.

Author Contributions: Visualization, M.F.; Conceptualization, M.F., P.M. and G.B.; Data curation, M.F., I.L., R.C., P.F., M.R.T., I.C. and T.S.; Formal analysis, M.F., P.M. and G.B.; Funding acquisition, P.M. and G.B.; Investigation, M.F., I.L., R.C., P.F., M.R.T., I.C. and T.S.; Methodology, M.F., P.M. and G.B.; Project administration, P.M. and G.B.; Supervision, P.M. and G.B.; Validation, M.F., P.M., I.L., R.C., P.F., M.R.T., I.C., T.S. and G.B.; Visualization, M.F.; Writing—original draft, M.F., I.L., R.C., P.F., M.R.T., I.C. and T.S.; Writing—review and editing, M.F., G.B. and P.M. All authors have read and agreed to the published version of the manuscript.

Funding: This research was funded by the Advanced Green Materials for Cultural Heritage (AGM for CuHe) project (MIUR PNR fund with code: ARS01_00697; CUP E66C18000380005).

Data Availability Statement: Data are contained within the article or Supplementary Materials.

Acknowledgments: The authors wish to thank La Bottega Calatina and Laquattro for having supplied ceramic wastes used as geopolymeric precursors. The authors also thank, for the support in measurements and investigation, Giuseppe Cultrone (Department of Mineralogy and Petrology, University of Granada—Spain), and CIC (Centro de Instrumentation Cientifica—University of Granada); Piero Baglioni and Emiliano Carretti (Department of Chemistry, University of Florence), and CSGI (Center for Colloid and Surface Science—Department of Chemistry, University of Florence); Carlo Alberto Garzonio (Department of Earth Science, University of Firenze) and Cristina Leonelli (Department of Engineering "Enzo Ferrari", University of Modena and Reggio Emilia).

Conflicts of Interest: The authors declare no conflict of interest.

References

1. Pathak, A.; Kumar, S.; Jha, V.K. Development of Building Material from Geopolymerization of Construction and Demolition Waste (CDW). *Trans. Indian Ceram. Soc.* **2014**, *73*, 133–137. [CrossRef]
2. Allaoui, D.; Nadi, M.; Hattani, F.; Majdoubi, H.; Haddaji, Y.; Mansouri, S.; Oumam, M.; Hannache, H.; Manoun, B. Eco-Friendly Geopolymer Concrete Based on Metakaolin and Ceramics Sanitaryware Wastes. *Ceram. Int.* **2022**, *48*, 34793–34802. [CrossRef]
3. Tan, J.; Cai, J.; Li, J. Recycling of Unseparated Construction and Demolition Waste (UCDW) through Geopolymer Technology. *Constr. Build. Mater.* **2022**, *341*, 127771. [CrossRef]
4. Reig, L.; Tashima, M.M.; Soriano, L.; Borrachero, M.V.; Monzó, J.; Payá, J. Alkaline Activation of Ceramic Waste Materials. *Waste Biomass Valoriz.* **2013**, *4*, 729–736. [CrossRef]
5. Robayo-Salazar, R.; Valencia-Saavedra, W.; de Gutiérrez, R.M. Reuse of Powders and Recycled Aggregates from Mixed Construction and Demolition Waste in Alkali-Activated Materials and Precast Concrete Units. *Sustainability* **2022**, *14*, 9685. [CrossRef]
6. Hwang, C.L.; Yehualaw, M.D.; Vo, D.H.; Huynh, T.P.; Largo, A. Performance Evaluation of Alkali Activated Mortar Containing High Volume of Waste Brick Powder Blended with Ground Granulated Blast Furnace Slag Cured at Ambient Temperature. *Constr. Build. Mater.* **2019**, *223*, 657–667. [CrossRef]
7. Wong, C.L.; Mo, K.H.; Yap, S.P.; Alengaram, U.J.; Ling, T.C. Potential Use of Brick Waste as Alternate Concrete-Making Materials: A Review. *J. Clean. Prod.* **2018**, *195*, 226–239. [CrossRef]
8. Panizza, M.; Natali, M.; Garbin, E.; Tamburini, S.; Secco, M. Assessment of Geopolymers with Construction and Demolition Waste (CDW) Aggregates as a Building Material. *Constr. Build. Mater.* **2018**, *181*, 119–133. [CrossRef]
9. Frittelloni, V. *Rapporto Rifiuti Speciali Edizione 2022*; Istituto Superiore per la Protezione e la Ricerca Ambientale: Rome, Italy, 2022; ISBN 9788844811167.
10. Sarkar, M.; Dana, K. Partial Replacement of Metakaolin with Red Ceramic Waste in Geopolymer. *Ceram. Int.* **2021**, *47*, 3473–3483. [CrossRef]
11. Mir, N.; Khan, S.A.; Kul, A.; Sahin, O.; Lachemi, M.; Sahmaran, M.; Koç, M. Life Cycle Assessment of Binary Recycled Ceramic Tile and Recycled Brick Waste-Based Geopolymers. *Clean. Mater.* **2022**, *5*, 100116. [CrossRef]
12. Bernal, S.A.; Rodríguez, E.D.; Kirchheim, A.P.; Provis, J.L. Management and Valorisation of Wastes through Use in Producing Alkali-Activated Cement Materials. *J. Chem. Technol. Biotechnol.* **2016**, *91*, 2365–2388. [CrossRef]
13. Almutairi, A.L.; Tayeh, B.A.; Adesina, A.; Isleem, H.F.; Zeyad, A.M. Potential Applications of Geopolymer Concrete in Construction: A Review. *Case Stud. Constr. Mater.* **2021**, *15*, e00733. [CrossRef]
14. Bassani, M.; Tefa, L.; Russo, A.; Palmero, P. Alkali-Activation of Recycled Construction and Demolition Waste Aggregate with No Added Binder. *Constr. Build. Mater.* **2019**, *205*, 398–413. [CrossRef]
15. Coletti, C.; Maritan, L.; Cultrone, G.; Mazzoli, C. Use of Industrial Ceramic Sludge in Brick Production: Effect on Aesthetic Quality and Physical Properties. *Constr. Build. Mater.* **2016**, *124*, 219–227. [CrossRef]
16. Fugazzotto, M.; Cultrone, G.; Mazzoleni, P.; Barone, G. Suitability of Ceramic Industrial Waste Recycling by Alkaline Activation for Use as Construction and Restoration Materials. *Ceram. Int.* **2023**, *49*, 9465–9478. [CrossRef]
17. Azevedo, A.R.G.; Vieira, C.M.F.; Ferreira, W.M.; Faria, K.C.P.; Pedroti, L.G.; Mendes, B.C. Potential Use of Ceramic Waste as Precursor in the Geopolymerization Reaction for the Production of Ceramic Roof Tiles. *J. Build. Eng.* **2020**, *29*, 101156. [CrossRef]
18. Van Deventer, J.S.J.; Provis, J.L.; Duxson, P.; Brice, D.G. Chemical Research and Climate Change as Drivers in the Commercial Adoption of Alkali Activated Materials. *Waste Biomass Valoriz.* **2010**, *1*, 145–155. [CrossRef]
19. Davidovits, J. Geopolymers—Inorganic Polymeric New Materials. *J. Therm. Anal.* **1991**, *37*, 1633–1656. [CrossRef]
20. Pachego-Torgal, F.; Labrincha, J.A.; Leonelli, C.; Palomo, A.; Chindaprasirt, P. *Handbook of Alkali-Activated Cements, Mortars and Concretes*; Elsevier: Cambridge, UK, 2015; ISBN 9781782422884.
21. Provis, J.L.; Bernal, S.A. Geopolymers and Related Alkali-Activated Materials. *Annu. Rev. Mater. Res.* **2014**, *44*, 299–327. [CrossRef]
22. Allahverdi, A.; Kani, E.N. Construction Wastes as Raw Materials for Geopolymer Binders. *Int. J. Civ. Eng.* **2009**, *7*, 154–160.

23. Albitar, M.; Mohamed Ali, M.S.; Visintin, P.; Drechsler, M. Durability Evaluation of Geopolymer and Conventional Concretes. *Constr. Build. Mater.* **2017**, *136*, 374–385. [CrossRef]
24. Alhawat, M.; Ashour, A.; Yildirim, G.; Aldemir, A.; Sahmaran, M. Properties of Geopolymers Sourced from Construction and Demolition Waste: A Review. *J. Build. Eng.* **2022**, *50*, 104104. [CrossRef]
25. Lancellotti, I.; Vezzali, V.; Barbieri, L.; Leonelli, C.; Grillenzoni, A. Construction and Demolition Waste (Cdw) Valorization in Alkali Activated Bricks. In *Wastes: Solutions, Treatments and Opportunities III*; Taylor and Francis Group: London, UK, 2020; pp. 495–499, ISBN 9780367257774.
26. Komnitsas, K.; Zaharaki, D.; Vlachou, A.; Bartzas, G.; Galetakis, M. Effect of Synthesis Parameters on the Quality of Construction and Demolition Wastes (CDW) Geopolymers. *Adv. Powder Technol.* **2015**, *26*, 368–376. [CrossRef]
27. Amin, S.K.; El-Sherbiny, S.A.; El-Magd, A.A.M.A.; Belal, A.; Abadir, M.F. Fabrication of Geopolymer Bricks Using Ceramic Dust Waste. *Constr. Build. Mater.* **2017**, *157*, 610–620. [CrossRef]
28. Leonelli, C.; Romagnoli, M. *Geopolimeri: Polimeri Inorganici Attivati Chimicamente*, 2nd ed.; ICerS: Bologna, Italy, 2013.
29. Duxson, P.; Fernández-Jiménez, A.; Provis, J.L.; Lukey, G.C.; Palomo, A.; Van Deventer, J.S.J. Geopolymer Technology: The Current State of the Art. *J. Mater. Sci.* **2007**, *42*, 2917–2933. [CrossRef]
30. Geraldes, C.F.M.; Lima, A.M.; Delgado-Rodrigues, J.; Mimoso, J.M.; Pereira, S.R.M. Geopolymers as Potential Repair Material in Tiles Conservation. *Appl. Phys. A Mater. Sci. Process.* **2016**, *122*, 197. [CrossRef]
31. Moutinho, S.; Costa, C.; Cerqueira, Â.; Rocha, F.; Velosa, A. Geopolymers and Polymers in the Conservation of Tile Facades. *Constr. Build. Mater.* **2019**, *197*, 175–184. [CrossRef]
32. Ricciotti, L.; Molino, A.J.; Roviello, V.; Chianese, E.; Cennamo, P.; Roviello, G. Geopolymer Composites for Potential Applications in Cultural Heritage. *Environments* **2017**, *4*, 91. [CrossRef]
33. Robayo, R.A.; Mulford, A.; Munera, J.; de Gutiérrez, R.M. Alternative Cements Based on Alkali-Activated Red Clay Brick Waste. *Constr. Build. Mater.* **2016**, *128*, 163–169. [CrossRef]
34. Rovnaník, P.; Rovnaníková, P.; Vyšvařil, M.; Grzeszczyk, S.; Janowska-Renkas, E. Rheological Properties and Microstructure of Binary Waste Red Brick Powder/Metakaolin Geopolymer. *Constr. Build. Mater.* **2018**, *188*, 924–933. [CrossRef]
35. Tuyan, M.; Andiç-Çakir, Ö.; Ramyar, K. Effect of Alkali Activator Concentration and Curing Condition on Strength and Microstructure of Waste Clay Brick Powder-Based Geopolymer. *Compos. Part B Eng.* **2018**, *135*, 242–252. [CrossRef]
36. Barone, G.; Caggiani, M.C.; Coccato, A.; Finocchiaro, C.; Fugazzotto, M.; Lanzafame, G.; Occhipinti, R.; Stroscio, A.; Mazzoleni, P. Geopolymer Production for Conservation-Restoration Using Sicilian Raw Materials: Feasibility Studies. *IOP Conf. Ser. Mater. Sci. Eng.* **2020**, *777*, 012001. [CrossRef]
37. Djobo, J.N.Y.; Tchadjié, L.N.; Tchakoute, H.K.; Kenne, B.B.D.; Elimbi, A.; Njopwouo, D. Synthesis of Geopolymer Composites from a Mixture of Volcanic Scoria and Metakaolin. *J. Asian Ceram. Soc.* **2014**, *2*, 387–398. [CrossRef]
38. Yip, C.; Lukey, G.C.; van Deventer, J.S.J. The Coexistence of Geopolymeric Gel and Calcium Silicate Hydrate at the Early Stage of Alkaline Activation. *Cem. Concr. Res.* **2005**, *35*, 1688–1697. [CrossRef]
39. Lancellotti, I.; Catauro, M.; Ponzoni, C.; Bollino, F.; Leonelli, C. Inorganic Polymers from Alkali Activation of Metakaolin: Effect of Setting and Curing on Structure. *J. Solid State Chem.* **2013**, *200*, 341–348. [CrossRef]
40. Ahmari, S.; Ren, X.; Toufigh, V.; Zhang, L. Production of Geopolymeric Binder from Blended Waste Concrete Powder and Fly Ash. *Constr. Build. Mater.* **2012**, *35*, 718–729. [CrossRef]
41. Reig, L.; Tashima, M.M.; Borrachero, M.V.; Monzó, J.; Cheeseman, C.R.; Payá, J. Properties and Microstructure of Alkali-Activated Red Clay Brick Waste. *Constr. Build. Mater.* **2013**, *43*, 98–106. [CrossRef]
42. Ruiz-Santaquiteria, C.; Fernández-Jiménez, A.; Skibsted, J.; Palomo, A. Clay Reactivity: Production of Alkali Activated Cements. *Appl. Clay Sci.* **2013**, *73*, 11–16. [CrossRef]
43. Fernández-Jiménez, A.; Palomo, A. Characterisation of Fly Ashes. Potential Reactivity as Alkaline Cements. *Fuel* **2003**, *82*, 2259–2265. [CrossRef]
44. Pulidori, E.; Lluveras-Tenorio, A.; Carosi, R.; Bernazzani, L.; Duce, C.; Pagnotta, S.; Lezzerini, M.; Barone, G.; Mazzoleni, P.; Tiné, M.R. Building Geopolymers for CuHe Part I: Thermal Properties of Raw Materials as Precursors for Geopolymers. *J. Therm. Anal. Calorim.* **2022**, *147*, 5323–5335. [CrossRef]
45. Pelosi, C.; Occhipinti, R.; Finocchiaro, C.; Lanzafame, G.; Pulidori, E.; Lezzerini, M.; Barone, G.; Mazzoleni, P.; Tiné, M.R. Thermal and Morphological Investigations of Alkali Activated Materials Based on Sicilian Volcanic Precursors (Italy). *Mater. Lett.* **2023**, *335*, 133773. [CrossRef]
46. *EN 1926 2006*; Natural Stone Test Methods—Determination of Uniaxial Compressive Strength. European Commission: Brussels, Belgium, 2006.
47. Buchwald, A.; Kaps, C.; Hohmann, M. Alkali-Activated Binders and Pozzolan Cement Binders—Compete Binder Reaction or Two Sides of the Same Story ? In Proceedings of the 11th International Congress on the Chemistry of Cement, Durban, South Africa, 11–16 May 2003; pp. 1238–1247.
48. Warr, L.N. IMA–CNMNC Approved Mineral Symbols. *Miner. Mag.* **2021**, *85*, 291–320. [CrossRef]
49. Lancellotti, I.; Ponzoni, C.; Barbieri, L.; Leonelli, C. Alkali Activation Processes for Incinerator Residues Management. *Waste Manag.* **2013**, *33*, 1740–1749. [CrossRef]
50. Xu, H.; Van Deventer, J.S.J. The Geopolymerisation of Alumino-Silicate Minerals. *Int. J. Miner. Process.* **2000**, *59*, 247–266. [CrossRef]

51. Mostafa, N.Y.; El-Hemaly, S.A.S.; Al-Wakeel, E.I.; El-Korashy, S.A.; Brown, P.W. Characterization and Evaluation of the Pozzolanic Activity of Egyptian Industrial By-Products: I: Silica Fume and Dealuminated Kaolin. *Cem. Concr. Res.* **2001**, *31*, 467–474. [CrossRef]
52. Panagiotopoulou, C.; Kontori, E.; Perraki, T.; Kakali, G. Dissolution of Aluminosilicate Minerals and By-Products in Alkaline Media. *J. Mater. Sci.* **2007**, *42*, 2967–2973. [CrossRef]
53. Fagerlund, G. Determination of Specific Surface by the BET Method. *Matériaux Constr.* **1973**, *6*, 239–245. [CrossRef]
54. Nazari, A.; Bagheri, A.; Riahi, S. Properties of Geopolymer with Seeded Fly Ash and Rice Husk Bark Ash. *Mater. Sci. Eng. A* **2011**, *528*, 7395–7401. [CrossRef]
55. Azevedo, A.G.D.S.; Strecker, K.; Lombardi, C.T. Produção de Geopolímeros à Base de Metacaulim e Cerâmica Vermelha. *Cerâmica* **2018**, *64*, 388–396. [CrossRef]
56. Komnitsas, K.; Zaharaki, D. Geopolymerisation: A Review and Prospects for the Minerals Industry. *Miner. Eng.* **2007**, *20*, 1261–1277. [CrossRef]
57. Pecchioni, E.; Fratini, F.; Cantisani, E. *Le Malte Antiche e Moderne Tra Tradizione Ed Innovazione*; Pàtron Editore: Bologna, Italy, 2008.
58. Pacheco-Torgal, F.; Tam, V.W.Y.; Labrincha, J.A.; Ding, Y.; de Brito, J. *Handbook of Recycled Concrete and Demolition Waste*; Woodhead Publishing: Cambridge, UK, 2013.
59. Rowles, M.R.; O'Connor, B.H. Chemical and Structural Microanalysis of Aluminosilicate Geopolymers Synthesized by Sodium Silicate Activation of Metakaolinite. *J. Am. Ceram. Soc.* **2009**, *92*, 2354–2361. [CrossRef]
60. Hassan, A.; Arif, M.; Shariq, M. Use of Geopolymer Concrete for a Cleaner and Sustainable Environment e A Review of Mechanical Properties and Microstructure. *J. Clean. Prod.* **2019**, *223*, 704–728. [CrossRef]
61. Fořt, J.; Vejmelková, E.; Koňáková, D.; Alblová, N.; Čáchová, M.; Keppert, M.; Rovnaníková, P.; Černý, R. Application of Waste Brick Powder in Alkali Activated Aluminosilicates: Functional and Environmental Aspects. *J. Clean. Prod.* **2018**, *194*, 714–725. [CrossRef]
62. Najafi Kani, E.; Allahverdi, A.; Provis, J.L. Efflorescence Control in Geopolymer Binders Based on Natural Pozzolan. *Cem. Concr. Compos.* **2012**, *34*, 25–33. [CrossRef]
63. Zhang, Z.; Provis, J.L.; Ma, X.; Reid, A.; Wang, H. Efflorescence and Subflorescence Induced Microstructural and Mechanical Evolution in Fly Ash-Based Geopolymers. *Cem. Concr. Compos.* **2018**, *92*, 165–177. [CrossRef]
64. Leonelli, C. Definizione, Preparazione, Proprietà Ed Applicazioni. In *Geopolimeri: Polimeri Inorganici Attivati Chimicamente*; Leonelli, C., Romagnoli, M., Eds.; ICerS: Bologna, Italy, 2013; pp. 1–22.
65. Sun, Z.; Cui, H.; An, H.; Tao, D.; Xu, Y.; Zhai, J.; Li, Q. Synthesis and Thermal Behavior of Geopolymer-Type Material from Waste Ceramic. *Constr. Build. Mater.* **2013**, *49*, 281–287. [CrossRef]